

## CHARACTERIZATION OF STRUCTURAL AND OPTICAL PROPERTIES OF AMORPHOUS CHALCOGENIDE (GeTe<sub>4</sub>)<sub>100-x</sub>In<sub>x</sub> (0≤x≤15) THIN FILMS

Y. A. EL-GENDY\*, A. M. SALEM

*Physics Department, Faculty of Science, Helwan University, Ain Helwan, Cairo, Egypt*

*Electron Microscope and thin films Department, National Research center, Cairo Egypt*

Nowadays, improve the optical properties of chalcogenide materials for optoelectronic applications became an important issue. In this work, amorphous chalcogenide (GeTe<sub>4</sub>)<sub>100-x</sub>In<sub>x</sub> (0≤x≤15) thin films systems have been prepared using an electron beam evaporation process. The amorphous state of the as-deposited films as well as the chemical compositions of the constituent elements was investigated using the X-ray diffraction and the energy dispersive x-ray spectroscopy (EDX). The transmission and reflection of the prepared films have been measured in the UV-Vis-NIR spectral range. Whereby, the optical constants of the as-deposited films *viz* the real and imaginary parts of the refractive indices, *n* and, *k*, beside the energy values of the optical band gap, *E<sub>g</sub>* were calculated using Murmann's exact equations. The average of the coordination number, cohesive energy of the bonds and the average heat of atomization were calculated for the investigated system. A correlation between these parameters and the optical band gap was elucidated.

(Received April 29, 2019; Accepted September 5, 2019)

*Keywords:* Thin films, Chalcogenide, Structure Properties, Optical properties.

### 1. Introduction

In the last few decades, most of the researches have been devoted to exploiting the amorphous as the promising candidate in various solid-state and, optoelectronic applications. Application of the amorphous chalcogenide in photovoltaic solar cells, optical data storage and, phase change memory have now great revolutions in various fields of technology [1-6]. A large of applications of the chalcogenide materials is owing to their optical properties, especially transmission in the infrared spectral range. In contrast to the amorphous chalcogenide materials, e.g. tellurium as a chalcogen-based element exhibits poor glass and unstable crystallization property [7, 8]. Hence, "Te" requires to combine with an additional of one or more of non-chalcogen elements like (Ge, Bi, Sn, Sb, In, etc.) with an appropriate ratio, to form stable glasses and provide further functionality, particularly in the field of transparent in the IR spectral region as well as for an optical data storage [9-17]. These additions lead to improve the characteristics properties of the chalcogenide materials for their applications.

Ge-Te chalcogenide thin film materials exhibit a reversible transition between crystalline and amorphous states [18-20]; where the optical properties of these two states have a considerable difference and the switching between them occurs very fast. On the other hand, many reports have been devoted to understanding the effects of the compositional variation and heat treatment on these materials properties and hence their practical applications in the case of addition of the third element to the Ge-Te glassy system. For instance, the physical properties of thin films corresponding to the ternary chalcogenide composition In-Sb-Te [12], Ge-Ga-Te [13-15], Ge-Te-Cu [16] Ge-Te-In [17] have been previously reported.

---

\*Corresponding authors: yassergendy2013@gmail.com

The lack of information on the structural and optical properties of the deposited  $(\text{GeTe}_4)_{100-x}\text{In}_x$  ( $0 \leq x \leq 15$ ) films, e.g. refractive index and its dispersion analysis at low absorption region prompt us to undertake this work. Moreover, a correlation between the structure, e.g. the mean coordination number,  $\langle Z \rangle$ , cohesive energy,  $\langle \text{CE} \rangle$ , the heat of atomization,  $\langle \text{Hs} \rangle$  and variation the energy of optical band gap have been elucidated.

## 2. Experimental

Bulk ingot alloys of the ternary compositions  $(\text{GeTe}_4)_{100-x}\text{In}_x$  ( $0 \leq x \leq 15$ ) has been prepared using melt quenching technique in vacuum sealed silica tubes at a pressure of  $10^{-3}$  Pa. High pure elements of Ge, In and Te of 6 N Sigma Aldrich were weighted according to their chemical formula. The tubes were heated in an electronic furnace according to a thermal program till 1273 K, and maintained at this temperature for 12 h; hereafter, the tubes were quenched rapidly in ice-cooled water to obtain amorphous alloys. The powdery samples from the prepared alloys were taken to evaporate the corresponding films at vacuum pressure of  $\sim 8 \times 10^{-3}$  Pa, via an e-beam evaporation system (Leybold-Heraeus Combifron CM-30, Germany). The deposition rate of  $4\text{--}6 \text{ nm s}^{-1}$  and thickness of the film were controlled during the evaporation process via thickness monitor (Edward model FTM5). Films of thickness around 500 nm deposited onto clean glass substrates at 300 K, have been chosen to study the properties of the films as typical samples due to the fact that thinner films of chalcogenide compositions would not yield profitable information at low absorption energy especially in UV range.

The X-ray diffraction of the prepared films were recorded employing an X-ray diffractometer (XRD) (Philips PW-1710) operating at 40 keV and 30 mA with monochromatic  $\text{CuK}\alpha$  radiation. The chemical compositions and morphology of the films were conducted using a scanning electron microscope (SEM) (Type JEOL model JEM-850). A dual beam spectrophotometer (Jasco, V-570, UV-VIS-NIR), at the normal incidence of light, was used to register the transmission and reflection spectra of the prepared films.

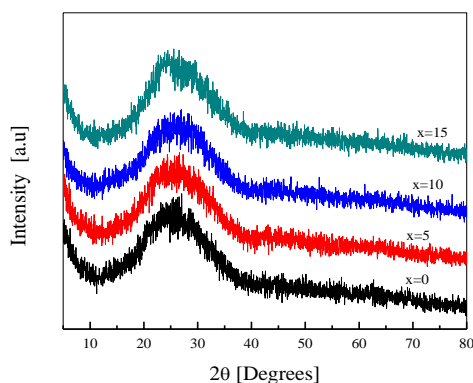


Fig. 1. X-ray diffraction patterns of as-deposited  $(\text{GeTe}_4)_{100-x}\text{In}_x$  thin film.

## 3. Results

### 3.1. Structure characterization

The X-ray diffraction for  $(\text{GeTe}_4)_{100-x}\text{In}_x$  ( $0 \leq x \leq 15$ ) films is shown in Fig. 1. The absence of any of sharp reflection peaks in the patterns confirms the amorphous state of the deposited films. The exact atomic percentage of the constituent elements of the deposited  $(\text{GeTe}_4)_{100-x}\text{In}_x$  ( $0 \leq x \leq 15$ ) films derived from the EDX analysis in comparison with the corresponding calculated nominal compositions, were summarized in Table 1. Fig. 2 a, b; illustrates the EDX patterns for two representative samples corresponding to  $x=0$  and 10. The results indicated the presence of peaks corresponding to Ge, Te, for the sample of  $x=0$ ; besides an "In" peaks for  $x=10$ ; no other reflection peaks corresponding to any of impurity elements are

presented. The peak observed at about 1.74 eV is attributed to the silicon element coming from the glass substrate. Inset of the figures shows the surface morphology of the films which has no feature confirmed the amorphous nature of the deposited films.

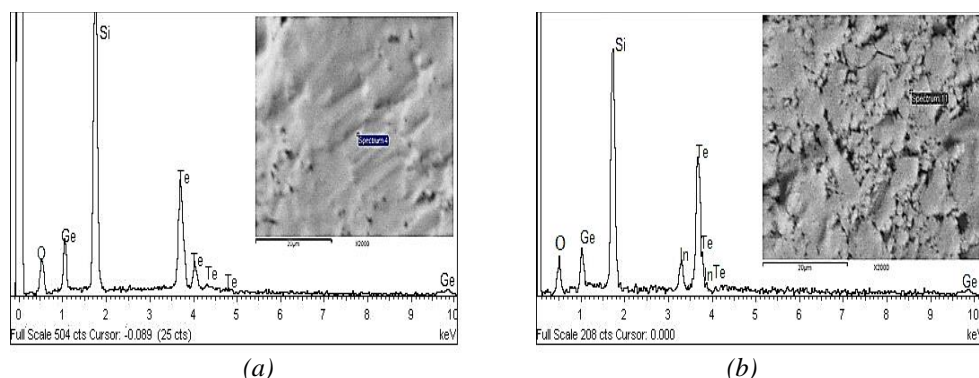


Fig. 2a, b EDX spectra of two representative  $(\text{GeTe}_4)_{100-x}\text{In}_x$  samples (a)  $x=0$  and (b)  $x=10$ . Inset depicts the corresponding scanning electron micrograph.

Table 1. EDX results and stoichiometric deviation parameter,  $R$  for  $(\text{GeTe}_4)_{100-x}\text{In}_x$  ( $0 \leq x \leq 15$ ) films.

Sample code	Calculated at. %			EDX results at. %			Exact formula	R
	Ge	Te	In	Ge	Te	In		
S1	20	80	0	21.04	78.96	0	$\text{Ge}_{21.04}\text{Te}_{78.96}$	1.876
S2	19	76	5	19.86	74.96	5.18	$\text{Ge}_{19.86}\text{Te}_{74.96}\text{In}_{5.18}$	1.578
S3	18	72	10	18.45	71.72	9.83	$\text{Ge}_{18.45}\text{Te}_{71.72}\text{In}_{9.83}$	1.389
S4	17	68	15	17.55	68.92	13.53	$\text{Ge}_{17.55}\text{Te}_{68.92}\text{In}_{13.53}$	1.244

### 3.2. Optical properties of the prepared $(\text{GeTe}_4)_{100-x}\text{In}_x$ ( $0 \leq x \leq 15$ ) films

The variation of the transmission  $T$  and reflection  $R$  spectrum *vs.* wavelength  $\lambda$  are shown in Fig. 3. The figures depict that, the transmission and reflection spectra exhibit interference fringes almost at the same wavelength position, indicates the uniformity of the film thickness. A redshift of the fundamental absorption edge towards lower energies was also observed as a result of increasing “In” content. At the longer wavelength *i.e.* in the transparent region the sum of the transmission and reflection are almost equal unity, indicates that no scattering or absorption occurs.

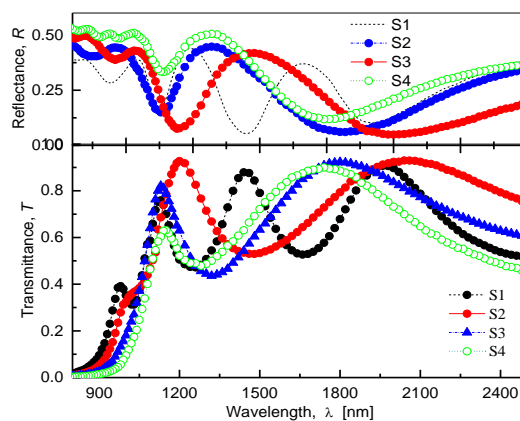


Fig. 3. Transmission and reflection spectra of as-deposited  $(\text{GeTe}_4)_{100-x}\text{In}_x$  thin films.

The refractive index,  $n$  and extinction coefficient,  $k$  of the films were calculated using a refined computer program based on the Murmann's exact equations [21, 22]. The program requires knowledge of primary values of both  $n$  and  $k$  to be run. These values can be calculated in the transparent region using the well-known Swanepoel relations [23]:

$$n_i = \sqrt{2s \frac{T_M - T_m}{T_M T_m} + \frac{s^2 + 1}{2} + \sqrt{\left(2s \frac{T_M - T_m}{T_M T_m} + \frac{s^2 + 1}{2}\right)^2 - s^2}} \quad (1)$$

where  $s$  is the refractive index of the glass substrate and  $T_M$  and  $T_m$  are the transmission maxima and minima, respectively. Utilizing the thickness of the film  $d$ , the primary values of the absorption coefficient,  $\alpha_i$ , could be calculated from the measurements of  $T(\lambda)$  and  $R(\lambda)$  using the relation [24]:

$$\alpha_i = \frac{1}{d} \ln \frac{(1-R^2)}{T} \quad (2)$$

Hence, the primary values of the extinction coefficient  $k_i = \alpha_i \lambda / 4\pi$  can be calculated.

Fig. 4a & b show the spectral variation of the refractive index,  $n$  and the extinction coefficient,  $k$  of  $(\text{GeTe}_4)_{100-x}\text{In}_x$  prepared films calculated on the basis of Murmann's exact equations. Fig. 4-a depict that, the refractive index,  $n$ , exhibits anomalous dispersion behavior in the fundamental absorption region *i.e* below  $\lambda < 1100 \text{ nm}$  (at the fundamental absorption edge). This behavior may be due to the effects of resonance between the incident electromagnetic radiation and the electron polarization [25, 26]. Behind the fundamental absorption edge,  $\lambda > 1100 \text{ nm}$ , the refractive index decreases as the wavelength increasing, exhibits normal behavior of dispersion. Additionally, in the anomalous dispersion region, the value of the refractive index at a fixed wavelength increases with increasing "In" content in the "Ge-Te" host matrix. In the other hand, the extinction coefficient,  $k$ , Fig. 4-b decreases with the increase in the wavelength and takes its lower values at  $\sim 1100$ .

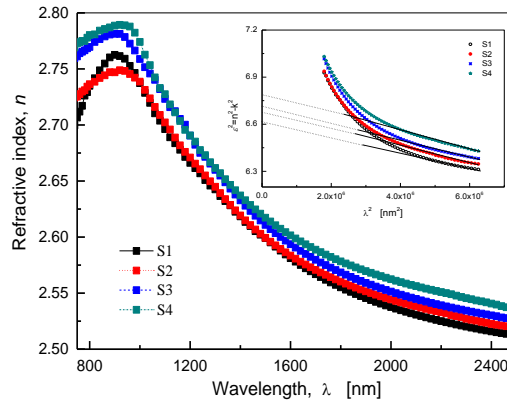


Fig. 4. a spectral variation of the refractive index of  $(\text{GeTe}_4)_{100-x}\text{In}_x$  thin films. Inset shows the plots of  $\epsilon_r = n^2 - k^2$ .

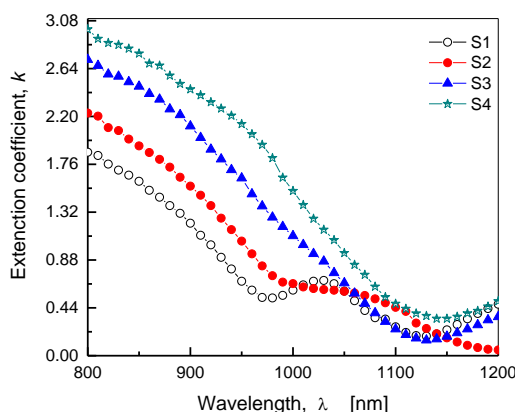


Fig. 4. b variation of the extinction coefficient vs. wavelength for the  $(\text{GeTe}_4)_{100-x}\text{In}_x$  thin films.

The dispersion of the refractive index in the normal dispersion region can be analyzed according to Spitzer and Fan model [27]:

$$\varepsilon_r = n^2 - k^2 = \varepsilon_\infty - A\lambda^2 \quad (3)$$

where,

$$A = \frac{e^2 N}{4\pi^2 c^2 \varepsilon_0 m^*}$$

where  $\varepsilon_r$  is the real part of the dielectric constant,  $\varepsilon_\infty$  high-frequency dielectric constant,  $e$  electron charge,  $c$  speed of light,  $\varepsilon_0$  permittivity of free space and  $N/m^*$  is the ratio of the carrier concentration to the effective mass. The inset of Fig. 4-a; depicts the spectral variation of  $\varepsilon_r$  against  $\lambda^2$  in the wavelength range 1400-2500 nm, by extrapolating the linear; one can obtain the values of  $\varepsilon_\infty$  and  $N/m^*$  from the intercept and slope of the curves, respectively. Furthermore, also in the transparency range, when the electron damping frequency,  $\gamma \ll \omega$  ( $\omega = 2\pi c/\lambda$  is the angular frequency) and  $n^2 \gg k^2$ , the real part of the dielectric constant obey the relation [28]:

$$\varepsilon_r = n^2 - k^2 = \varepsilon_\infty - \omega_p^2/\omega^2 \quad (4)$$

where  $\omega_p$  is the plasma frequency given by:

$$\omega_p^2 = \frac{e^2 \cdot N/m^*}{\varepsilon_0}$$

The  $\varepsilon_\infty$ , and  $N/m^*$  values as well as the plasma frequency,  $\omega_p$  for the ternary  $(\text{GeTe})_{100-x}\text{In}_x$  thin films system are summarized in Table 2. The determined values of  $\varepsilon_\infty$ ,  $N/m^*$ , and the plasma frequency  $\omega_p$  were found to increases with increasing "In" content at % in the Ge-Te host matrix. The finding can be attributed probably due to increasing the scattering effect of the free carrier concentration of the ionized impurities which reflects a reduction in the optical band gap.

Table 2. Optical properties of  $(\text{GeTe}_4)_{100-x}\text{In}_x$  thin films.

Sample code	Film thickness, $t$ [nm]	$\varepsilon_\infty$	$n = \sqrt{\varepsilon_\infty}$	$N/m^*$ [ $\times 10^{55} m^{-3} kg^{-1}$ ]	$\omega_p$ [ $\times 10^{14}$ Hz]	$E_g$ [eV]
S1	543	6.613	2.572	1.82	2.29	1.17
S2	562	6.675	2.584	1.95	2.38	1.08
S3	517	6.722	2.593	2.04	2.44	1.02
S4	535	6.801	2.608	2.21	2.53	0.97

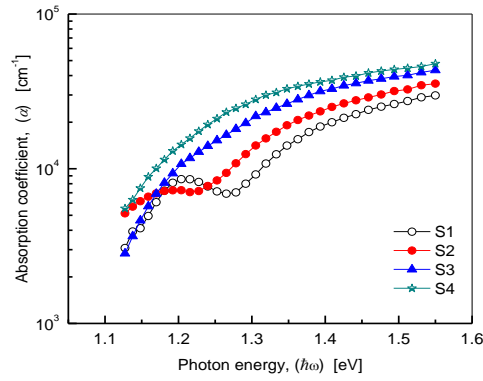


Fig. 5. Absorption coefficient,  $\alpha$ , vs. photon energy.

Fig. 5 illustrates the variation of the absorption coefficient,  $\alpha$  calculated on the basis of Murmann's exact equations as a function of the photon energy,  $(\hbar\omega)$ . It was found that  $\alpha$  as the energy of the photon increases, reaches to a value higher than  $10^4 \text{ cm}^{-1}$  in the photon energy range 1.1–1.55 eV. On the basis of the generally reasonable indirect optical transition model proposed by Tauc for amorphous semiconductor materials; the photon energy dependence of the absorption coefficient obeys the relation [29].

$$(\alpha\hbar\omega) = A(\hbar\omega - E_g) \quad (5)$$

where  $A$  is a constant parameter and  $E_g$  is the band gap energy. Fig. 6 depicts the variation of  $(\alpha\hbar\omega)^{1/2}$  vs.  $(\hbar\omega)$ . A linear fit of the of such curves to zero absorption, one can determine the values  $E_g$ , which summarized in Table 2. It was found that there is a shortage in the band gap energy, with increasing the “In” content in Ge-Te as a host matrix. The values of the optical band gap determined in this work are in context well with the corresponding values obtained for thermally evaporated  $(\text{GeTe}_4)_{100-x}\text{In}_x$  compositions [30].

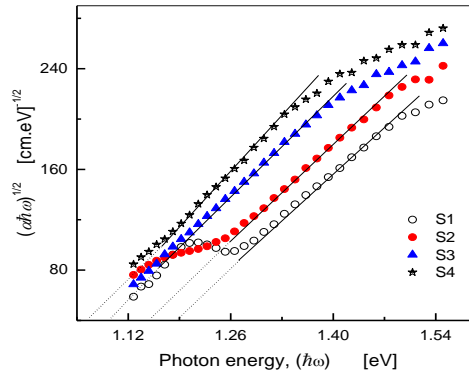


Fig. 6. A plots of  $(\alpha\hbar\omega)^{1/2}$  for the as-deposited  $(\text{GeTe}_4)_{100-x}\text{In}_x$  thin films.

#### 4. Discussion

The nature of the chalcogenide materials can be classified using the stoichiometric deviation parameter,  $R$  given by [31].

$$R = \frac{yN_{Te}}{xN_{In} + zN_{Ge}} \quad (6)$$

where  $x$ ,  $y$ , and  $z$  are the exact *at.%* of *In*, *Te* and *Ge* elements, and  $N_{Te}$ ,  $N_{In}$  and  $N_{Ge}$  are their atomic coordination number, respectively. The value of  $R$  in the chalcogenide systems can be classified into three different categories;  $R=1$  for a stoichiometric composition since only heteropolar bonds present *i.e.* chalcogen–chalcogen bonds,  $R>1$  for the case of chalcogen system rich, while  $R<1$  for the poor chalcogen system [32]. In the present work  $R>1$  (see Table 1); indicates that the investigated ternary systems belong to the chalcogen rich.

Within the scope of our knowledge, the various properties of the binary and ternary chalcogenide systems strongly depend on their chemical compositions and appear to vary according to their average coordination number  $\langle Z \rangle$  [33, 34]. This dependence reflects a clue about the presence of mechanical and chemical thresholds proven composition in these materials. It has been assured for many of the chalcogenide materials properties display an extreme at  $\langle Z \rangle = 2.40$  at which there is a conversion from under-constrained floppy network to over-constrained rigid network [35]; where with this number, it is supposed that the network attains its maximum stability. Further, according to Angell's concept [36, 37], where, the average coordination number,  $\langle Z \rangle$  can be classified into three distinct categories. (i) an under-constrained system at which the numbers of degree of freedom exceeds the numbers of constraints where  $\langle Z \rangle$  increases from 2 up to 2.4 which corresponding to thermodynamically and kinetically strong system; (ii) An over-constrained system where the numbers of constraints exceeds the numbers of degrees of freedom at which  $\langle Z \rangle$  increases from 2.421 to 2.757; that makes the system thermodynamically fragile but kinetically strong; and (iii) a deficiency in the chalcogen system at which the increase of  $\langle Z \rangle$  above 2.67 leads to a thermodynamically strong but kinetically fragile system [33]. The average numbers of coordination  $\langle Z \rangle$  for the compositions investigated in this work can be calculated according to the 8–N rule, where N is the outer-shell electrons according to the relation [34]:

$$\langle Z \rangle = 8 - \frac{4z+6y+3x}{100} \quad (7)$$

where, 3, 6 and 4 are the number of the outer shell electrons of *In*, *Te* and *Ge*, respectively, and  $x$ ,  $y$ , and  $z$  are the corresponding *at.%*. The values of  $Z$  for our investigated compositions listed in Table 3 varies in the range of 2.42-2.757; which indicates that system goes from thermodynamically fragile and kinetically strong system, (for the samples corresponding to  $Z$  in the range 2.42-to 2.664); to a thermodynamically strong but a kinetically fragile system, for the sample of  $Z>2.757$ .

Another two important parameters connected to the physical properties of the chalcogenide materials, namely, the  $CE$  and  $H_s$ . According to the chemical bond approach model (CBA) [35]; the heteronuclear bonds are more favored over homonuclear bonds, and the bonds are formed in a way that the bonds with higher energy are firstly formed and subsequently formation of bonds of lower energy, until all of the vacancy atoms available in the system are totally occupied. The heteronuclear bond energy can be calculated using the well-known Pauling principle as follows [35]:

$$D(A - B) = [D(A - A)D(B - B)]^{1/2} + 30(\chi_A - \chi_B)^2 \quad (8)$$

here,  $D(A-B)$  is the energy of the heteronuclear bond,  $D(A-A)$  and  $D(B-B)$  are the energy of the homonuclear bonds.  $\chi_A$  and  $\chi_B$  are the electronegativity of the elements A and B, respectively; using the values of the homonuclear bonds energies of 37.6, 33 and 24.2  $kcal.mol^{-1}$  corresponding to *Ge*, *Te* and *In* bonds [36,37]; one can calculate the energy of the heteronuclear *Ge-Te*, *In-Te* bonds; which are 36.67 and 31.33  $kcal.mol^{-1}$ , respectively. Hence, the cohesive energy,  $CE$  of the ternary system was computed by adding the energies of the bonds present in the composition using [38]:

$$CE = \sum C_i E_i / 100 \quad \text{in } kcal.mol^{-1} \quad (9)$$

$C_i$  and  $E_i$  are the number of the expected chemical bonds in the system and the energy corresponding of each bond, respectively. The average heat of atomization,  $H_s$  of the studied compositions can be calculated using the relation [39, 40].

$$H_s = \frac{zH_s^{Ge} + yH_s^{Te} + xH_s^{In}}{z+y+x} \quad (10)$$

where  $H_s^{Ge} = 377$ ,  $H_s^{Te} = 197$  and  $H_s^{In} = 231.8 \text{ kJmol}^{-1}$  corresponding to the heat of atomization of *Ge*, *Te* and *In* elements, respectively, and  $z$ ,  $y$  and,  $x$  are their respective at%. The relative fraction of the chemical bonds formed, cohesive energy,  $\langle CE \rangle$ , heat of atomization,  $H_s$  as well as the average single bond energy,  $H_s/\langle Z \rangle$  for the studied compositions are in Table 3. The data in table 3 depicts that, with increasing the "In" content, the relative fractions of Ge-Te and Te-Te bonds decrease at the expense of increasing the In-Te bonds. In the other side, both of  $\langle CE \rangle$ ,  $H_s$  and,  $H_s/\langle Z \rangle$  decreases with increasing the "In" content at. %, while the average coordination numbers,  $Z$  increases.

Table 3. Structure parameters of  $(GeTe_4)_{100-x}In_x$  ( $0 \leq x \leq 15$ ) ternary system.

Sample code	Z	Distribution of the formed chemical bonds			CE	$H_s$	$H_s/\langle Z \rangle$
		Ge-Te	In-Te	Te-Te			
S1	2.421	0.5329	0	0.4671	34.956	234.872	97.015
S2	2.553	0.5298	0.1037	0.3665	34.772	234.551	91.873
S3	2.664	0.5146	0.2055	0.2799	34.545	233.631	87.699
S4	2.757	0.5093	0.2945	0.1962	34.377	233.299	84.621

To understand the decrease of the value of optical gap with the addition of "In" to the Ge-Te as a host matrix, it is interesting to correlate the variation of  $E_g$  with the chemical bond energy using an empirical relationship viable for semiconductors of the diamond and other Zinc-blende structure given by [41, 42]:

$$E_g = a(H_s - b) \quad (11)$$

where "a" and "b" are special constants. This relation proposed that the average heat of atomization,  $H_s$  has the same trend of  $E_g$ . According to Yamaguchi [43], the relation can be utilized also to the amorphous chalcogenide systems. Fig. 7 depicts a graphical representation of  $H_s$  and  $E_g$  as a function of the average coordination numbers,  $\langle Z \rangle$ , where both  $E_g$  and  $H_s$  exhibit the same trend in agreement with the above-suggested relation.

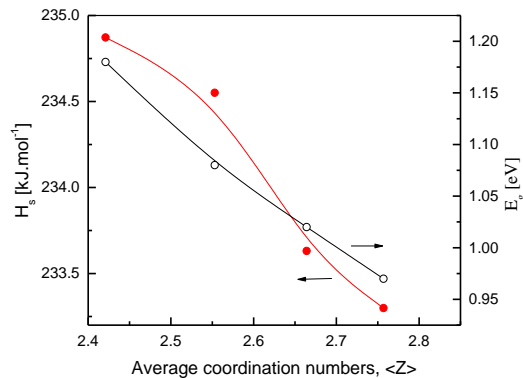


Fig. 7. Variation of the optical band gap and heat of atomization vs. average coordination numbers,  $\langle Z \rangle$ .

## 5. Conclusions

In this work, the structural and compositional dependence of the optical properties of  $(\text{GeTe}_4)_{100-x}\text{In}_x$  ( $0 \leq x \leq 15$ ) films prepared by electron beam evaporation process have been investigated. The amorphous nature of the films prepared at room temperature has been confirmed by X-ray and scanning electron micrograph. The constituent elements of the deposited films have been studied using the energy dispersive X-ray spectroscopy. The optical constants of the as-deposited films determined using the Murmann's exact equations reflect intention of the refractive index with the intention the “In” content at the expense of Ge-Te content. The dispersion of the refractive indices in the low absorption region was analyzed according to Spitzer and Fan model.

The calculated values of the high-frequency dielectric constant,  $\epsilon_\infty$ , ratio of the carriers concentration to the effective mass,  $N/m^*$ , and the plasma frequency,  $\omega_p$  were found to increase with increasing the “In” content, while the optical gap decreases. An increase of the “In” content in the Ge-Te in the host matrix reflects an increase in the average coordination numbers, which leads to transfer the system from thermodynamically fragile and kinetically strong to a system of thermodynamically strong but a kinetically fragile. The values of the cohesive energy, the heat of atomization, as well as the average single bond energy of the system, decreases with increasing the “In” content.

## References

- [1] A. Zakery, S. R. Elliott, J. Non-Cryst. Solids **330**, 1 (2003).
- [2] E. M. Vinod, R. Naik, A. P. A. Faiyas, R. Ganesan, K. S. Sangunni, J. Non-Cryst. Solids **356**, 2172 (2010).
- [3] K. A. Aly, J. Non-Crystalline Solids **355**, 1489 (2009).
- [4] G. X. Wang, Q. H. Nie, X. Shen, F. Chen; Vacuum **86**, 1572 (2012).
- [5] A. A. Bahgat, E. M. Mahmoud, A. S. Abd Rabo, A. Mahdy Iman, J. Mater. Sci. **41**, 3451 (2006).
- [6] S. A. Kozyukhin, A. I. Popov, E. N. Voronkov, Thin Solid Films **518**, 5656 (2010).
- [7] X. Zhang, H. Ma, C. Blanchetière, J. Lucas, J. Non-Cryst. Solids **161**, 327 (1993).
- [8] J. Kalb, M. Wuttig, F. Spaepen, J. Mater. Res. **22**, 748 (2007).
- [9] E. Carria, J. Electrochem. Soc. **159**, H130 (2012).
- [10] H. Shen, S. Lee, J. Kang, T. Eom, S. Han, Journal of Alloys and Compounds, **767**, 522 (2018).
- [11] Yaqi Zhng, Materials Letters **194**, 149 (2017).
- [12] Vitaliy Bilovol, J. Non-Crystalline Solids **447**, 315 (2016).
- [13] Ning Dong, J. Infrared Physics & Technology **86**, 181 (2017).
- [14] Y. A. El-Gendy, J. Physics D: Applied Physics **42**, 115408 (2009).
- [15] V. Nemeč, M. Nazabal, H. L. Ma. Dussauze, X. Bouyrie, X. H. Zhang, Thin Solid Films **531**, 454 (2013).
- [16] N. El-Kabany, A. H. Oraby, Ga. AL-Zaidy, Solid State Sciences **27**, 11 (2014).
- [17] Yonghui Wang, Fen Chen, Xiang Shen, Shixun Dai, Qiuhua Nie, Infrared Physics Technology **60**, 335 (2013).
- [18] W. Hoyer, I. Kaban, P. Jovari, E. Dost, J. Non-Cryst. Solids **338–340**, 565 (2004).
- [19] Pál Jóvári, Andrea Piarristeguy, Annie Pradel, Ildikó Pethes, Roman Chernikov; Journal of Alloys and Compounds **771**, 268 (2019).
- [20] A. C. Galca, F. Sava, I. D. Simandan, C. Bucur, V. Dumitru, C. Porosnicu, C. Mihai, A. Velea, Journal of Non-Crystalline Solids **499**, 1 (2018).
- [21] O. S. Heavens, “Optical Properties of Thin Solid Films” Dover, New York, 1965.
- [22] O. S. Heavens, in: G. Hass, R. Thus (Eds.), “Physics of Thin Films”, Academic Press, New York, 1964.
- [23] R. Swanepoel, J. Phys. E Sci. Instrum. **16**, 1214 (1983).
- [24] J. I. Pankove, “Optical Processes in Semiconductors”, Prentice-Hall, New Jersey,

- 1971, P. 93.
- [25] M. M. El-Nahass, I. T. Zedan, F. S. Abu-Samah, *Optics & Laser Technology* **44**, 621 (2012).
- [26] A. S. Hassanien, Alaa A. Akl; *Journal of Alloys and Compounds* **648**, 280 (2015).
- [27] W. G. Spitzer, H.Y. Fan, *Phys. Rev.* **106**, 882 (1957).
- [28] A. Osama, M. M. Abdel-Aziz, I. S. Yahia, *Appl. Surf. Sci.* **255**, 4829 (2006).
- [29] Tauc, R. Grigorovici, A. Vancu; *Phys. Status Solidi (b)* **15**, 627 (1966).
- [30] A Zaidan, V Ivanova, P Petkov, *Journal of Physics: Conference Series* **356**, 012014 (2012).
- [31] L. Tichy, H. Ticha, *Matt. Lett.* **21**, 313 (1994).
- [32] L. Tichy, H. Ticha, *J. Non Cryst. Solids* **189**, 141 (1995).
- [33] Omar A. Lafi, Mousa M.A. Imran; *Journal of Alloys and Compounds* **509**, 5090 (2011).
- [34] G. Saffarini, A. Schlieper, *Appl. Phys. A* **61**, 29 (1995).
- [35] J. C. Phillips, M. F. Thorpe, *Solid State Commun.* **53**, 699 (1985).
- [36] Arpit Kaistha, V. S. Rangra, Pankaj Sharma; *Glass Physics and Chemistry* **41**, 175 (2015).
- [37] R. Sharma, S. Sharma, P. Kumar, R. Thangaraj, M. Mian, *Journal of Non-Crystalline Solids* **459**, 13 (2017).
- [38] Ambika, P. B. Barman, *Physica B* **405**, 822 (2010).
- [39] H. Rawan, K. Anup, S. Raman *Journal of Ovonic Research* **8**, 29 (2012).
- [40] A. Kaisth, V. S. Rangr, P. Sharma, *Glass Phys. Chem.* **41**, 175 (2015).
- [41] P. Aigrain, M. Balkanski, *Selected Constant Relative to Semiconductors*, Pergamon Press, New York, 1961.
- [42] H. MahfozKot, Farid M. Abdel-Rahim; *Materials Science in Semiconductor Processing* **38**, 209 (2015).
- [43] M. Yamaguchi, *Philos. Mag. B* **51**, 6651 (1985).